THE UNIVERSITY *of* EDINBURGH

Edinburgh Research Explorer

COMPUTED TOMOGRAPHIC ANATOMY AND CHARACTERISTICS OF RESPIRATORY ASPERGILLOSIS IN JUVENILE WHOOPING CRANES

OPEN ACCESS

COMPUTED TOMOGRAPHIC ANATOMY AND CHARACTERISTICS OF RESPIRATORY ASPERGILLOSIS IN JUVENILE WHOOPING CRANES

TOBIAS SCHWARZ, CRISTIN KELLEY, MARIE E. PINKERTON, BARRY K. HARTUP

Respiratory diseases are a leading cause of morbidity and mortality in captivity reared, endangered whooping cranes (*Grus americana*). Objectives of this retrospective, case series, cross-sectional study were to describe computed tomography (CT) respiratory anatomy in a juvenile whooping crane without respiratory disease, compare CT characteristics with gross pathologic characteristics in a group of juvenile whooping cranes with respiratory aspergillosis, and test associations between the number of CT tracheal bends and bird sex and age. A total of 10 juvenile whooping cranes (one control, nine affected) were included. Seven affected cranes had CT characteristics of unilateral extrapulmonary bronchial occlusion or wall thickening, and seven cranes had luminal occlusion of the intrapulmonary primary or secondary bronchi. Air sac membrane thickening was observed in three cranes in the cranial and caudal thoracic air sacs, and air sac diverticulum opacification was observed in four cranes. Necropsy lesions consisted of severe, subacute to chronic, focally extensive granulomatous pathology of the trachea, primary bronchi, lungs, or air sacs. No false positive CT scan results were documented. Seven instances of false negative CT scan results occurred; six of these consisted of subtle, mild air sacculitis including membrane opacification or thickening, or the presence of small plaques found at necropsy. The number of CT tracheal bends was associated with bird age but not sex. Findings supported the use of CT as a diagnostic test for avian species with respiratory disease and tracheal coiling or elongated tracheae where endoscopic evaluation is impractical. © 2015 The Authors. *Veterinary Radiology & Ultrasound* published by Wiley Periodicals, Inc. on behalf of American College of Veterinary Radiology.

Key words: aspergillosis, CT, Gruiformes, Grus americana, respiratory anatomy.

Introduction

THE NEAR EXTINCTION OF THE WHOOPING crane (*Grus americana*) remains one of the most widely known case studies in conservation.[1] Since 1993 reintroduction of juvenile cranes produced at captive propagation centers has been used in the species recovery program. The goal of reintroduction is to establish additional self-sustaining breeding populations in North America, thereby minimizing the possibility of loss of the species through natural disaster or disease outbreak. Whooping cranes, however, experience numerous challenges to breeding and survival in captivity that may limit the success of captive propagation for reintroduction. Respiratory diseases are a leading cause of morbidity and mortality in captive-reared whooping cranes.[2–4] Current recovery efforts for whooping cranes rely on developing new populations, rather than supplementation of existing populations, as a hedge against extinction. With high annual costs of captive propagation, management emphasis has been on maximizing production of juvenile whooping cranes suitable for reintroduction. The long-lived, low reproductive capacity of wild whooping cranes demands rapid production of a genetically diverse pool of individuals to reach demographic goals in reintroduced populations. Application of advanced diagnostic techniques with a high degree of reliability, though expensive, may help to limit some of the problems in whooping crane management. These include ineffective treatments dedicated to individuals with chronic diseases and a low probability of reintroduction or future contribution to captive breeding. The anatomy of the whooping crane poses unique challenges to imaging and diagnosis of respiratory pathology. Superimposition of soft tissue structures on radiographs commonly interferes with delineation of lesions within the trachea, bronchi, air sacs, and lungs unless disease is advanced. The trachea of whooping cranes is extremely

long (up to 1.5 m in length) and convoluted within the sternum,[5–7] rendering endoscopic approach to the tracheal bifurcation (syrinx) impractical and localization of obstructive disease very difficult.

Computed tomography (CT) has been used with increasing success to image the avian respiratory system, both in order to establish normal anatomy[8,9] and to diagnose pathology, primarily of the upper respiratory tract.[10–12] Computed tomography eliminates superimposition of structures and can therefore aid in accurately evaluating the unique aspects of avian respiratory anatomy.[12–16] It may be especially useful in imaging and localizing lesions of the trachea, syrinx, and primary bronchi of birds.[15,16] Computed tomography evaluations have proven successful in the diagnosis of mycotic pneumonic infections or compressions or calcification of the air sacs of psittacine birds.[13–16]

To our knowledge, no CT study of cranes or other comparative species with unusual tracheal anatomy has been published (e.g., cracids, guinea fowl, spoonbills, or swans). The objectives of our retrospective, case series, cross-sectional study were to describe CT features of respiratory anatomy in a normal juvenile whooping crane, compare CT characteristics with necropsy findings in a group of juvenile whooping cranes with confirmed aspergillosis, and test the hypothesis that the number of CT tracheal bends would be associated with age but not sex of the cranes.

Materials and Methods

Case Selection

Medical records at the University of Wisconsin Veterinary Medical Teaching Hospital and the International Crane Foundation were searched for whooping crane patients that received an intra vitam CT examination of their respiratory system and a complete necropsy examination. Inclusion criteria for the study included intra vitam CT examination of the respiratory tract of whooping cranes of diagnostic quality, necropsy or surgical exploration within 4 h of the CT examination, and histology or culture for fungal organisms. Diagnostic quality CT scans were defined as those including the trachea from the level of the furcula (fused clavicle) to the caudal aspect of the lungs and caudal air sacs. For all included birds, the following medical data were collected: age at CT examination in days, sex, clinical history and presentation, reason for CT examination, anesthetic protocol, postmortem examination, and histopathology. Because the decision to euthanize these endangered birds was based on the CT diagnosis at the time, all reviewers were implicitly aware of the fact that there was significant pathology identified on CT. The presence or absence of lesions described from CT and necropsy was tallied among six anatomic regions in all cases: trachea (cervical and intrasternal portions), syrinx, primary bronchi, lung,

cranial air sacs (cervical, clavicular, and cranial thoracic), and caudal air sacs (caudal thoracic and abdominal).

Computed Tomography Data Recorded

The following CT parameters were recorded: kilovoltage, tube current, tube rotation time, axial or helical scan mode, slice width and pitch, image reconstruction algorithm frequency (low/medium/high), and total scan duration. All CT studies were retrospectively reviewed by a board-certified veterinary radiologist (T.S.), who was unaware of any details of the necropsy diagnosis. Images were evaluated using dedicated DICOM viewer software (Osirix, Geneva, Switzerland, version 5.8.5-64 bit) on a computer workstation (Apple Mac Pro, Apple) with a calibrated LCD flat screen monitor (Apple Cinemax Display, 30 inch, Apple). During the course of image evaluation, multiplanar reconstructions and variable windowing were used according to the preferences of the viewer. The following anatomic and pathologic features were scored subjectively as follows: tracheal ring anatomy (open or closed rings), cross-sectional shape (circular or oval), degree and location of tracheal intrasternal coiling (number of bends), tracheal wall mineralization, thickening, and luminal fluid accumulation (absent/mild/marked); syrinx and primary and secondary bronchial anatomy (extra- and intrapulmonary, air sac insertion), bronchial occlusion (location, longitudinal extent, maximal degree of luminal obstruction), dilatation, distortion, and wall thickening; parenchymal lung density (air-filled, soft tissue infiltrate); air sac and diverticula identification and pathology (wall thickening, presence of luminal fluid or soft tissue); and nonrespiratory pathology. Respiratory anatomy was evaluated using standard avian anatomical references.[17–19] Tracheal coiling was quantified in bends. A bend was defined as a section of trachea with a 90° unidirectional tracheal long-axis change. If a long-axis directional change occurred before the 90° angle point, any reached curvature angle above 45° was recorded as a half bend (Fig. 1). The sternal tracheal entrance and exit points and the spatial relationship of the bends were recorded. Mean lung density in Hounsfield units (HU) was measured on a transverse CT image at level of the caudal scapular margin that was free of any motion artifacts for each lung using a region of interest (ROI) tool. A 6-mm-diameter ROI tool was placed in a consistent manner over the dorsolateral aspect of each lung avoiding large vascular or airway structures or any visibly abnormal density (Fig. 2). The ROI size and shape was made identical for both lungs by copying and pasting the tool.

Statistical Analysis

Statistical analyses were selected and performed by the first author (T.S.) with commercially available statistical
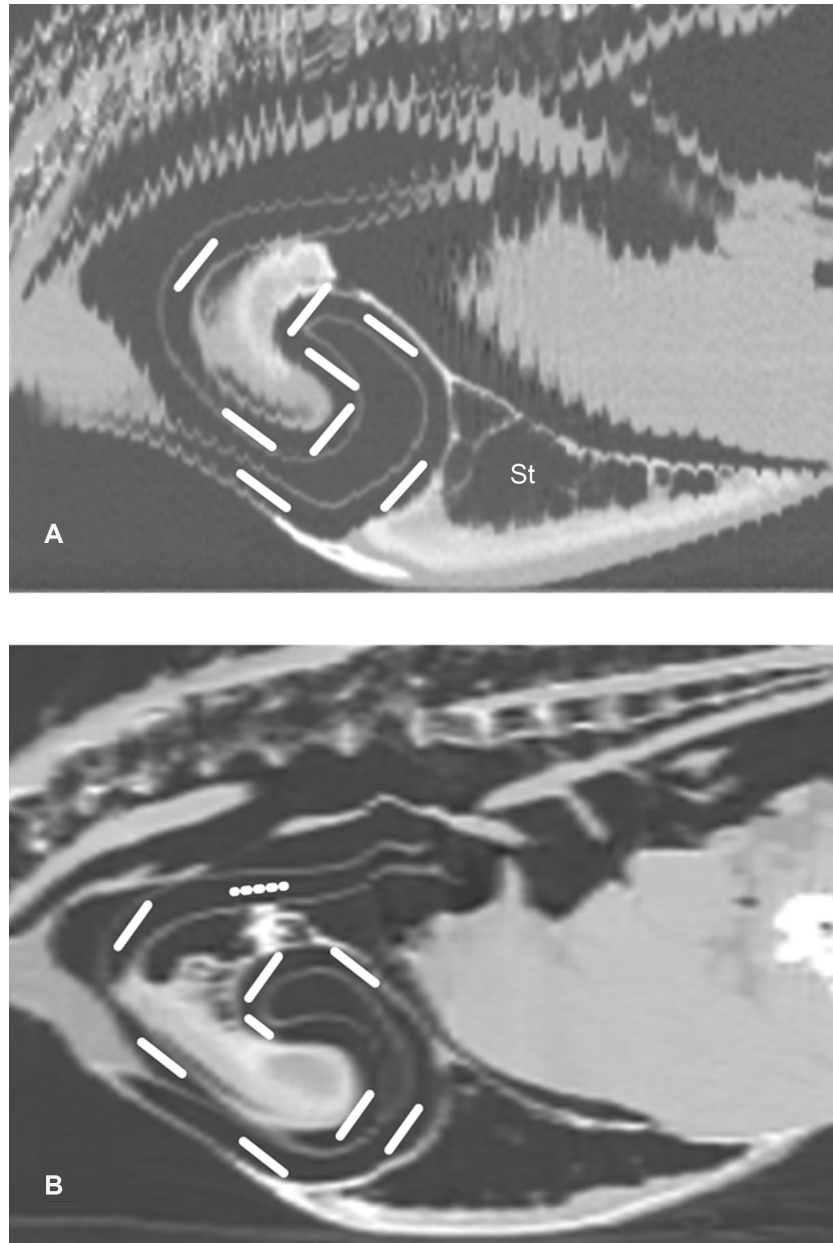
FIG. 1. Sagittally reformatted CT images of intrasternal tracheal coiling in two whooping cranes with a total of 7 (A, case 6, 72 days old) and 7.5 bends (B, case 10, 117 days old). The full white bars represent the perpendicular tracheal long axis based on which the number of bends was calculated (dotted bar = half bend). The pneumatized carina of the sternum (St) that is housing the tracheal coils is easily visible. The jagged appearance is due to respiratory motion artifact.

software (Minitab, v17, Minitab Inc., Coventry, UK). Continuous variables were expressed as mean ± standard deviation. Level of significance was set as $P < 0.05$. The association between sex and number of CT tracheal bends was examined with the Mann–Whitney test. The association between age and the number of CT tracheal bends was examined with a simple linear regression test. The mean CT lung density in HU was calculated for each bird of both lungs and for all birds left lungs, right lungs, and for all lungs.

Results

Clinical Findings

Ten whooping cranes met the inclusion criteria (six males and four females). All cranes had been captive-reared at the International Crane Foundation or referred to this facility from the Necedah National Wildlife Refuge, Necedah, WI, USA while undergoing reintroduction to the wild.[20] The median age of the cranes was 66 days (mean = 109 days, range 35–317 days). Nine of 10 cranes presented with
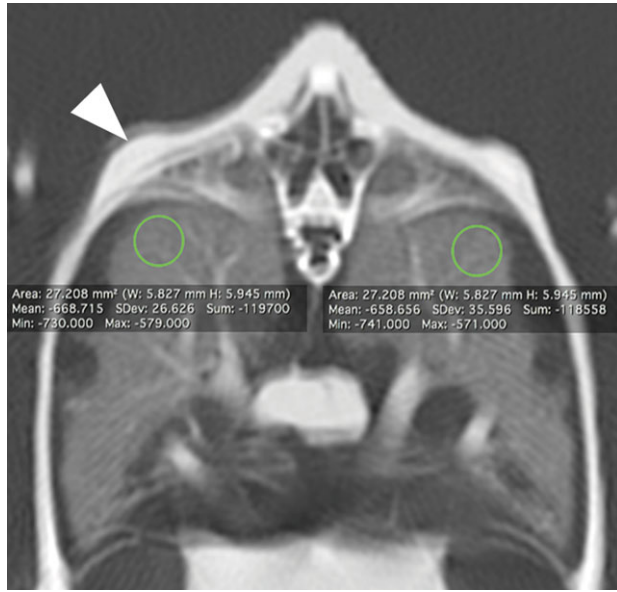
FIG. 2. Computed tomography (CT) image of the coelom of a 35-day-old whooping crane (case 8) at the level of the caudal scapula (arrowhead). A region of interest tool (green circles) has been placed in the dorsolateral lung for measurement of mean lung density in Hounsfield units.

clinical signs of respiratory disease, including voice change or loss, wheezing, moist rales, dyspnea, and/or cyanosis. The median duration of clinical signs prior to CT evaluation was 43 days (mean = 87 days, range 9–268 days). Despite the slowly progressive nature of the disease in most cases, no cranes showed weight loss or significant developmental problems. The 10th case presented with a fractured lateral cnemial crest of the right tibiotarsus but no discernable respiratory disease.

Computed Tomography Protocols and Findings

All studies had been performed on a helical single-detector row CT unit (GE Hi Speed LXI® and GE Hi-Light Advantage®, GE Medical Systems, Milwaukee, WI) under isoflurane anesthesia. Computed tomography examinations were performed with a slice width of 1–5 mm (mean 4 mm), 80 or 120 kV peak tube voltage, 80–280 mAs tube current, 0.8–2 s tube rotation time, and a total series duration of 35–480 s (mean 165 s). Four examinations were performed in sequential mode (pitch = 0) and the remaining six in helical mode (pitch = 1.4). In four cases, an additional series covering a smaller area of suspected abnormalities observed on the initial series was performed with a lower slice width and pitch. Computed tomography images were generated using a reconstruction algorithm of high spatial frequency and additional reconstructions in some cases.

Computed tomographic evaluation of the trachea showed complete tracheal rings in all cranes and an oval cross-sectional shape of the cervical portion and circular shape of the intrasternal and coelomic trachea. There was intra- and parasternal tracheal coiling in all cranes with a mean of 6.95 bends (range 4–10 bends) (Fig. 1). There was no significant difference in the median and spread of the number of tracheal bends between male and female cranes ($P = 0.9138$). There was a statistically significant positive linear relationship between age in days and number of tracheal bends ($t = 5.76$, $P < 0.001$, $R^2 = 0.8056$). The course and location of tracheal loops was consistent in all birds. At the level of the clavicles, the trachea entered the pneumatized carina of the sternum via a cranially widely open communication with the unpaired clavicular air sac. Inside the sternum the trachea looped along the outer ventral, then caudal and then dorsal margins of the sternal air sac diverticulum. If there was more extensive coiling the trachea then coiled in an S-shaped manner in the central area of the diverticulum. Only the last cranially oriented bend exited the carina on the left side, remained medial to the clavicle and looped craniad, then dorsad, then caudad toward the syrinx in all cranes. One crane showed extensive mineralization of the intrasternal trachea and a small amount of luminal fluid pooling. The syrinx and the primary bronchi were identified in all cranes. There was no syringeal bulla or marked luminal widening of the syrinx compared to the trachea (described as *tympanum* in other bird species).

The primary bronchi emanated from the syrinx with a slit-shaped cross-section, consisting of a rigid cartilaginous lateral aspect and a flexible medial aspect (the vocal elastic membranes). The slit shape and the thinner medial wall were visible in CT in all normal primary bronchi. The pessulus could not be identified as a distinct triangular cartilage. The syrinx and extrapulmonary bronchi were abnormal in seven cranes. Six cranes had a unilateral complete primary bronchial occlusion, extending through the entire extrapulmonary portion, causing bronchial dilatation and distortion (Fig. 3). One crane showed a distinct unilateral wall thickening of the extrapulmonary bronchus. The intrapulmonary portion of the primary bronchus could be followed through the lungs to its termination in the abdominal air sac.

Several intrapulmonary secondary bronchi could be identified in all cranes, but only the lateroventral secondary bronchus could be identified specifically, based on its termination into the caudal thoracic air sac. Pathological changes in the intrapulmonary primary or secondary bronchi were detected in seven cranes, consisting of complete luminal occlusion with soft tissue material (Fig. 4). Mean density of all lungs was −664.24 HU (range −741.22 to −602.45 HU).

At least portions of all air sacs were evaluated in each crane, although the caudal extent of the abdominal air sacs was not included in all CT scans. The clavicular air sac was
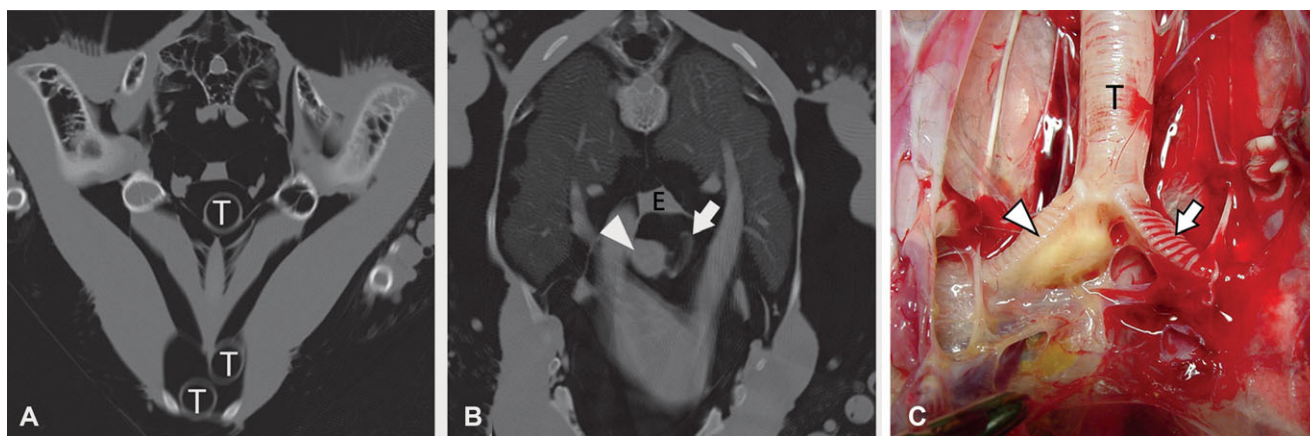
Fig. 3. Computed tomography (CT) images (A and B) and corresponding necropsy photograph (C) of the trachea and the extrapulmonary portion of the emanating primary bronchi in a 66-day-old whooping crane (case 3). The normal left primary bronchus (arrow) is slit-shaped in cross-section with a thick cartilaginous lateral wall and a thinner medial vocal membrane. The right primary bronchus (arrowhead) is markedly distended and filled with soft tissue material to the level of the lung. The arrowhead is superimposed on the aortic arch. E, esophagus.

septated cranially in all cranes. The following diverticula were identified: axillary, sternal, coracoid, scapular (all but two cranes), and humeral. Air sac membrane thickening was observed in three cranes in the cranial and caudal thoracic air sacs (Fig. 5), and air sac diverticulum opacification was observed in four cranes (one coracoid, one scapular, and three humeral).

Nonrespiratory lesions were observed in four cranes and included clavicular ($n = 1$), rib ($n = 2$), and tibiotarsal ($n = 1$) bone fractures as well as subcutaneous emphysema ($n = 1$).

Necropsy Protocol and Findings

A complete gross necropsy within 4 h after the CT examination had been performed or reviewed in all affected cases by one author (M.P.) who was not aware of details of the CT examination. A single case was evaluated via partial pneumonectomy, which also occurred within 4 h after the CT examination had been performed by one author (B.H.) who was unaware of details of the CT examination. Samples of representative tissues and pathologic lesions (including brain, heart, lung, trachea, primary bronchi, air sac membrane(s), liver, kidney, spleen, thyroid gland, adrenal gland, esophagus, proventriculus, ventriculus, and intestine) were fixed in 10% buffered formalin, paraffin embedded, sectioned at 4 μm, and stained with hematoxylin and eosin for light microscopy. Sections of tissues containing granulomatous lesions were stained with Gomori methenamine silver to confirm fungal organisms and/or submitted for routine fungal culture at the VMTH.

Culture and histological evaluation of pathological lesions confirmed *Aspergillus fumigatus* or unspeciated *Aspergillus sp.* infection in nine cranes. Lesions consisted variously of severe, subacute to chronic, focally exten-

sive granulomatous inflammation of the trachea, primary bronchi, lungs, or air sacs. Mild, chronic granulomatous air sacculitis was identified in the remaining crane without antemortem respiratory signs, but no etiology was determined.

In 49 of 56 (87.5%) possible pairwise comparisons, CT scan results were verified by necropsy results (Appendix 1). Lesions observed at necropsy typically consisted of small (several mm) to large (cm+) granulomas characterized as moderate to severe. No false positive CT scan results were documented. Seven instances of false negative CT scan results occurred. In one case, a moderately sized bronchial lesion infiltrated the lung parenchyma but the intrapulmonary extent was not identified from the CT scan. The six remaining false negative results consisted of subtle, mild forms of air sacculitis including mild-to-moderate membrane opacification or thickening, or the presence of 1–2 mm diameter (but $\leq$1 mm thick) plaques.

Discussion

The CT anatomic detail and diagnostic yield were very high in this study, likely due to the large size of the birds. However, this study revealed six false negative instances of air sac pathology determined from CT. We attribute these findings to the small size and limited distribution of the lesions. In addition, respiratory motion and a resulting slice mismatch artifact could not be controlled in the anesthetized cranes and may have contributed to the failure to detect the pulmonary disease noted at necropsy in case 4. These limitations would likely be minimized with modern multislice CT technology.

Aspergillosis lesions seem to occur in major airways and throughout the lungs in whooping cranes, as opposed to air sacs often observed in some gallinaceous and psittacine
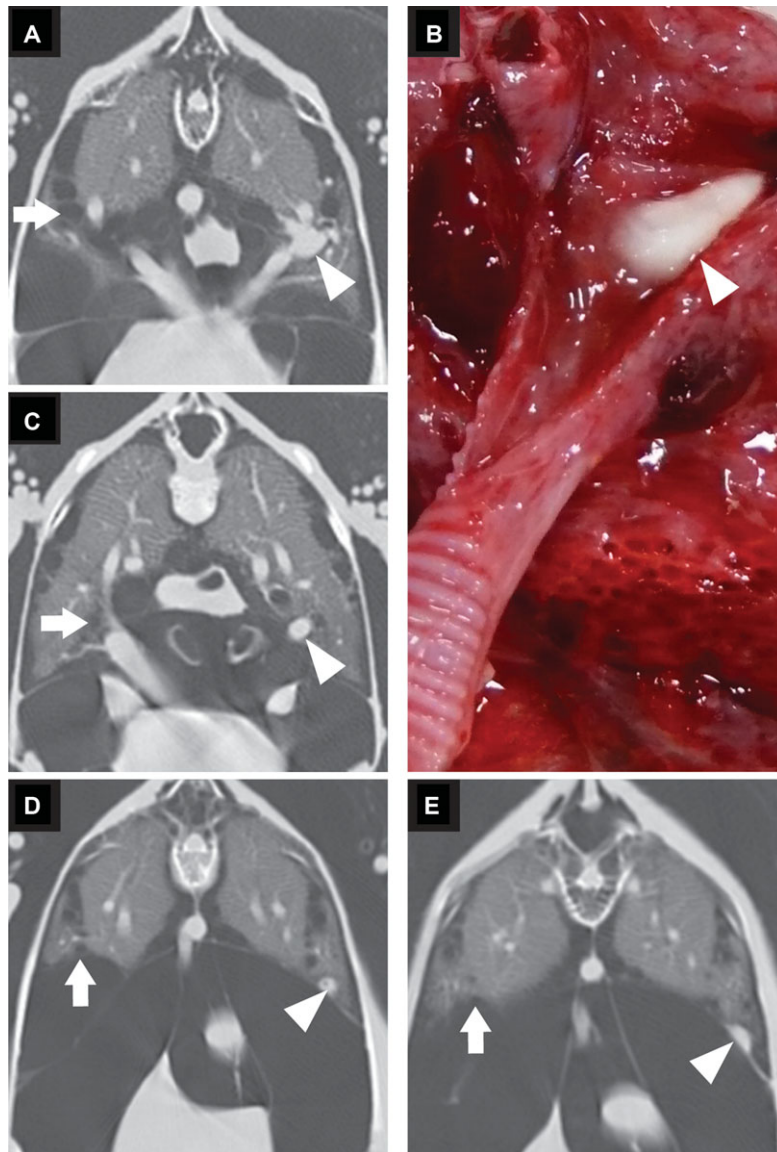
FIG. 4. Computed tomography (CT) images (A, C, and D) and corresponding necropsy photograph (B) of the occluded left lateroventral secondary bronchus (arrowheads) in a 50-day-old whooping crane (case 7) from its origin at the primary bronchus (A and B) via the caudal lung (C and D) to its entrance into the caudal thoracic airsac (E). Notice the similar course of the normal right lateroventral secondary bronchus (arrows). The true tubular shape of the bronchial obstruction is best appreciated in (B), whereas selected transverse CT images in (A, C, and E) give it a nodular appearance.

species.[13] Tracheal convolution and exaggerated length results in increased airflow turbulence and dead space,[7] where aspirated material or microorganisms may settle, inciting disease. Diagnosis of syringeal mycosis or foreign body is accomplished in birds with linear tracheas via direct visualization using rigid or flexible endoscopy.[21,22] Because of the extreme length and convolution of a crane's trachea, endoscopy to the level of the syrinx is impossible without a surgical approach. Computed tomography allowed the inspection of anatomic regions such as the distal trachea, syrinx, and various diverticula that were inaccessible by standard means in live birds.

Computed tomographic imaging of living cranes in this study revealed unique aspects of whooping crane respiratory anatomy and allowed detailed inspection of anatomic sites inaccessible by other modalities. We depicted anatomic features of intrapulmonary primary and secondary bronchi using CT and diagnosed bronchial obstruction leading to specific air sacs, information not reported previously to our knowledge. The ontogeny of tracheal coiling was documented among the cranes of various ages in the study, offering an opportunity to further understand the development of this adaptation for the production of loud, penetrating calls as adults.[6,7] We also believe CT could be
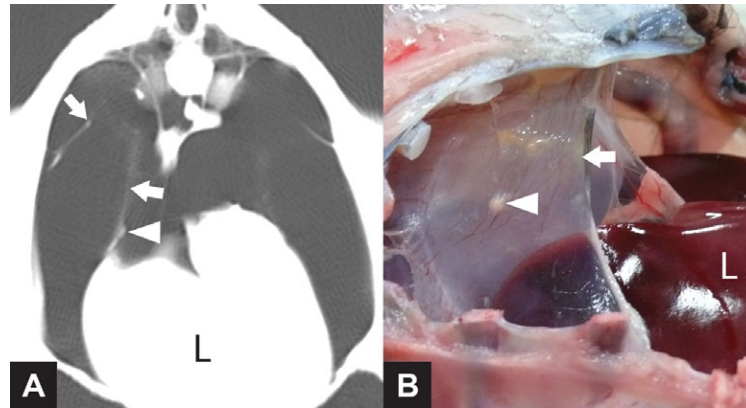
Fig. 5. Computed tomography image (A) and corresponding necropsy photograph (B) of the right caudal thoracic air sac in a 35-day-old whooping crane (case 8). The air sac membrane (arrows) shows mild diffuse and nodular (arrowheads) thickening. The normally translucent membrane is opaque on necropsy. L, liver.

successfully applied to the diagnostic evaluation of other avian species with tracheal coiling or unusual respiratory anatomy. Findings supported our hypothesis that the coiling of the whooping crane trachea would be age- but not sex-dependent. This is of clinical interest because predicting the degree of tracheal coiling may allow selection in the field of very young whooping cranes with respiratory disease for advanced diagnostic and treatment procedures, where orotracheal endoscopic access might still be possible. The lung density values in our study (mean −664.24 HU, range −741.22 to −602.45 HU) were close to the mean, but wider in range than those published in healthy psittacine birds such as the African grey parrot (*Psittacus erithacus*, mean −621.32 HU, range −628.95 to −611.5 HU) and the Orange winged Amazon (*Amazona amazonica*, mean −630.85 HU, range −635.16 to −619.43 HU).[23] The wider range may be related to the primary bronchial occlusion in many cranes, thereby creating abnormal aeration of the lungs or be related to species-specific differences.

Our study had several limitations. Owing to the fact that the whooping crane is an endangered species and that these birds belong to a very resource-intense animal population, our sample size had to remain very limited. It could not be justified to perform the diagnostic procedure in disease-free birds. The study was performed on two different CT scanners with slightly different imaging protocols and with relatively long scan times by modern standards. However, the technical differences were relatively limited, and the airway structures were still well visible. It is likely that with modern multislice CT particularly the air sac wall could

be better assessed and false negative result rates could be reduced.

In conclusion, CT allowed detailed description of respiratory aspergillosis lesions in this sample of juvenile whooping cranes and accurately detected the locations of most necropsy lesions. Findings supported the use of CT for the diagnostic work up of suspected respiratory pathology in whooping cranes or other birds of similar size and in particular in avian species with tracheal coiling or elongated tracheae where endoscopic evaluation is impractical.

APPENDIX 1

Comparison of granulomatous respiratory lesion detection in six anatomic locations from CT scans and gross necropsies of whooping cranes

Case No.	Trachea	Syrinx	Primary	Lung bronchi	Cranial air sacs	Caudal air sacs
1	−/−*	+/+	+/+	−/−	−/−	−/−
2[†]	−/na	−/na	−/na	+/+	−/−	−/na
3	−/−	−/−	+/+	+/+	+/+	−/−
4[‡]	−/−	−/−	+/+	−/+	−/−	−/−
5	−/−	−/−	+/+	+/+	−/+	−/−
6	−/−	−/−	+/+	+/+	+/+	+/+
7	−/−	−/−	−/−	+/+	−/+	−/+
8	−/−	−/−	−/−	+/+	−/+	+/+
9	−/−	−/−	+/+	+/+	−/+	+/+
10	−/−	−/−	−/−	−/−	−/+	−/−

*CT scan lesion detection / lesion detected at gross necropsy.
[†]Only lungs and cranial air sacs were evaluated in this case.
[‡]Trachea and syrinx were evaluated grossly via endoscopy in this case.
na, not applicable; −, not detected; +, detected.

REFERENCES

1. Meine CD, Archibald GW. The cranes: status survey and conservation action plan. Gland, Switzerland: IUCN, 1996.

2. Carpenter JW, Derrickson SR. Whooping crane mortality at the Patuxent Wildlife Research Center, 1966–1981. Proceedings of the 3rd North American Crane Workshop, 1982;175–179.

3. Olsen GH, Taylor JA, Gee GF. Whooping crane mortality at Patuxent Wildlife Research Center, 1982–1995. Proceedings of the 7th North American Crane Workshop, 1997;243–248.

4. Hartup BK, Niemuth JN, Fitzpatrick B, et al. Morbidity and mortality of captive whooping cranes at the International Crane Foundation 1976–2008. Proceedings of the 11th North American Crane Workshop, 2010; 183–185.

5. Roberts TS. The convolution of the trachea in the sandhill and whooping cranes. Am Nat 1880;14:108–114.

6. Archibald GW. The unison call of cranes as a useful taxonomic tool. PhD dissertation. Ithaca, NY: Cornell University, 1977.

7. Gaunt AS, Gaunt SLL, Prange HD, et al. The effects of tracheal coiling on the vocalizations of cranes (Aves; Gruidae). J Comp Physiol A 1987;161:43–58.

8. Artmann A, Henninger W. Psittacine paranasal sinus – a new definition of compartments. J Zoo Wildl Med 2001;32:447–458.

9. Krautwald-Junghanns ME, Schumacher F, Sohn HG. The use of computer assisted tomography as an instrument in collecting information on anatomical structures of the respiratory tract in live birds. Zoology 1998;101:139–147.

10. Krautwald-Junghanns ME, Kostka VM, Dorsch B. Comparative studies on the diagnostic value of conventional radiography and computed tomography in evaluating the heads of psittacine and raptorial birds. J Avian Med Surg 1998;12:149–157.

11. Rosenthal K, Stefanacci J, Quesenberry K, et al. Computerized tomography in 10 cases of avian intracranial disease. Proc Ann Conf Assoc Avian Vet 1995;16:305.

12. Gumpenberger M. Chapter 49: Avian. In: Schwarz T, Saunders J (eds).Veterinary computed tomography. Chichester, UK: Wiley-Blackwell, 2011;517–532.

13. Krautwald-Junghanns ME, Schumacher F, Tellhelm B. Evaluation of the lower respiratory tract in Psittacines using radiology and computed tomography. Vet Radiol Ultrasound 1993;34:382–390.

14. Gumpenberger M, Henninger W. The use of computed tomography in avian and reptile medicine. Semin Avian Exotic Pet Med 2001;10:174–180.

15. Newell SM, Roberts GD, Bennett RA. Imaging techniques for avian lower respiratory diseases. Semin Avian Exotic Pet Med 1997;6:180–186.

16. Gumpenberger M, Scope A. CT diagnoses in avians suffering from upper respiratory tract disease. Proceedings of EVDI Annual Conference, Utrecht, The Netherlands, 2014; 27–30, p58.

17. Vollmerhaus B, Sinowatz F. Atmungsapparat. In: Sinowatz F, Frewein J, Waibl H (eds): Lehrbuch der Anatomie der Haustiere, Bd. 5. Anatomie der Vögel, 2nd ed. Berlin, Germany: Verlag Paul Parey, 1992;159–176.

18. Maina JN. The lung-air sac system of birds. Berlin, Germany: Springer-Verlag, 2005;1–210.

19. König HE, Navarro M, Zengerling G, et al. Atmungsapparat (apparatus respiratorius). In: König HE, Korbel R, Liebich HG (eds): Anatomie der Vögel – Klinische Aspekte und Propädeutik, 2nd ed. Stuttgart, Germany: Verlag Schattauer, 2009;127–140.

20. Hartup BK, Olsen GH, Czekala NM. Fecal corticoid monitoring in whooping cranes (Grus americana) undergoing reintroduction. Zoo Biol 2005;24:15–28.

21. Taylor M. Endoscopic diagnosis of avian respiratory tract diseases. Semin Avian Exotic Pet Med 1997;6:187–194.

22. Jones MP, Orosz SE. The diagnosis of aspergillosis in birds. Semin Avian Exotic Pet Med 2000;9:52–58.

23. Krautwald-Junghanns ME. Computertomographie des aviären Respirationstraktes. Berlin, Germany: Blackwell Wissenschafts-Verlag, 1997; 57–152.